

# Finite Element Analysis for Prediction of Shear and Stress Concentration & Distribution in Femoral Bone

N Suhendra, D Gustiono, E A Nugroho, Masmui, H Yuliani

Agency for the Assessment and Application of Technology, Puspiptek Distric 224<sup>nd</sup> Bld,  
Serpong – South Tangerang – Banten Indonesia

E-mail : [nandang.suhendra@bppt.go.id](mailto:nandang.suhendra@bppt.go.id)

**Abstract.** The effect of micromotion on the shear shielding and size of yielding region in the bone asperity in contact with metal of femoral stem was investigated. The main objective of this work was to gain an understanding of bone wear particle formation mechanism from the two-dimensional finite element model of cementless femoral stem type. To assess the influence of the parameters of interest, different friction coefficients and sliding distance (micromotion) were used in the numerical simulations. Results from the finite element analysis showed that the increase of the yielding region is strongly influenced by the rise in sliding distance (micromotion), which is related to the generation of bone wear particle formations. Finite element bone wear particle formation model, based on strain discontinuities, was therefore proposed for further works. The results obtained in this study can lead to the development of an accurate finite element wear particle formation mechanism model that would be of use in the assessment of an artificial implant performance and their development.

## 1. Introduction

Normal human joint performance is facilitated by low-friction articular cartilage bearing surfaces, which are conforming and self-regenerating[1-4]. Severely damage of natural joints, e.g. due to osteoarthritis, they are often replaced by artificial implants. The most common material combinations used for articulating surfaces in a total hip joint replacement are: metal - metal, metal - ultra high molecular weight polyethylene (UHMWPE), ceramic – ceramic and ceramic – UHMWPE[1, 3, 5-7]. Meanwhile, materials used for femoral stem are stainless steel, Titanium Alloys and recently polymeric composites.

Commonly, artificial hip joint designs utilizing a Titanium Alloys femoral stem, can last 20 years in the human body without failure[8]. However, there are several factors which affect the durability of the total hip joint prosthesis, one of which is implant – femoral bone contacting surface wear (and related phenomena)[9]. It is postulated that micromotion occurring within the interface of the implant and femoral bone premature failure of hip joint prostheses [8, 10, 11]. Micromotion of femoral stem from the bone surface was found to initiate aseptic loosening and early failure of the prosthesis[10, 12-16]. After reviewing the literature, one can conclude that, in some cases, roughened stems have been shown to fail earlier than polished stems of the same implant[16].

Herberts et al[17] analyzed the in-vivo failure behavior of a stem with a surface roughness of  $R_a=2\text{ }\mu\text{m}$ . They concluded that the stem was not stable and generated excessive osteolysis, particularly



around defects in the cement mantle. Based on this observation, it was suggested that under similar conditions such as number of cycles, load, stop to stop sequence and activity level, the harder counter-face roughness is the most important factor in both wear volume and the number of wear particles generated from the softer bone surfaces[18].

It was suggested that migration of prosthesis is defined as a change in position of prosthesis, cement mantle or both and is thought to indicate implant failure and represent loosening[19]. Once migration has begun, stability is lost and periprosthetic particles may modulate latter stages of loosening[19]. Mechanisms by which migration occurs are not fully understood. It could be due to fatigue failure of cancellous bone surrounding the prosthesis[20] leading to loss of osteo-integration of a stable prosthesis, or it could be attributed to surgical techniques—for example, reaming which disturbs capillary circulation of periprosthetic bone, leading to necrosis. The initial use of cement with first generation cementing technique allowed defects and stresses to occur within the cement which resulted in a weaker bone–cement interface and permitted the ingress of polyethylene particles, thus resulting in loosening[20]. With improved cementing techniques which include the use of a medullary plug, a cement gun, lavage of the canal, pressurisation, centralisation of the stem, and reduction in porosity in the cement, the incidence of femoral lysis has been reduced[20].

Attempts to reduce wear in order to prevent bone resorption have been made by incorporating hard bearing surfaces, i.e. metal-on-metal and ceramic-on-ceramic prostheses [21]. Apart from the improvement in the lubricating quality of the joint, a reduction in sliding distance was also expected to be beneficial in minimizing the rate of volumetric wear. The use of a smaller, up to a certain value, femoral head radius was another solution suggested [22].

Processes contributing to wear of cancellous bone in total hip arthroplasty (THA) are associated with surface features and the overall geometrical conformity of the mating components [3, 23, 24]. Therefore, it is important to understand the relationship between the microscopic wear mechanism, material properties such as: contact loading, surface roughness, etc. The loaded contact during micro-motion with sliding between two asperities can result in local elastic-plastic deformation, development and extension of microscopic cracks[25].

In general, there are two approaches that are used in simulation studies of wear. Damage arising from a single, isolated asperity contact can be studied[25-27], or alternatively the wear resulting from contacts between multiple asperities is considered[18, 28]. The first approach involves numerical modelling the movement of a hard asperity of known geometry over a specimen surface, resulting in wear, while the second approach is mainly experimental, using specially prepared specimens and a tribometer, such as a joint simulator.

Information about wear mechanisms involved in generation of wear particles of particular sizes during articulation has been well documented[5, 28-31]. However, details of the mechanisms by which particles separate from the parent material, caused by sliding contact in THA, are still being investigated. These processes are difficult to study in a laboratory environment, and consequently computer modelling must be used to advance our knowledge of such systems. The interlocking asperities of the cancellous bone surface and its harder counter-face (Titanium Alloys surface) are modelled using a simple geometry so that deformation and stresses distribution, and their effects on failure and wear mechanisms of cancellous bone in THA, can be identified.

In this work possible wear particle generation mechanisms in a Cancellous bone in a total hip joint prosthesis under sliding conditions were investigated using a 2-D finite element computational model. The aim of the study conducted was to develop the model that could be used to predict the effects of load, geometry and material properties on the stress and strain distributions occurring within the structure of hip joint replacement components. Prediction of mechanisms involved in the formation of cancellous bone wear particles is of the main objective of this study.

## **2. Experimental method**

### **2.1. Finite Element Geometrical Model**

A finite element model of the contact between two asperities has been developed. A contact between a single Titanium Alloy asperity (representing the femoral stem) and a single Cancellous bone asperity (representing the femoral bone) in the interlocking position was modelled. The scale of the model is of the order of micrometer size. Illustration of asperity geometrical scale is shown in Figure 1.

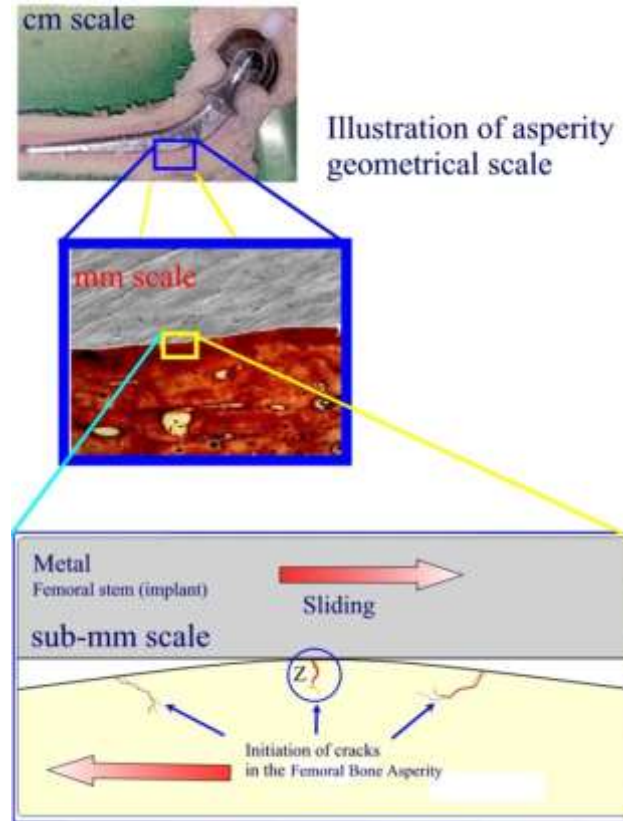


Figure 1: Illustration of Asperity Geomterical Scale

It was suggested by Fisher et al [32] that the real peak-to-valley height,  $R_t$ , of asperities on femoral stems are about  $0.07 - 0.08 \mu\text{m}$ . However, average asperity size of the well finished stem components is about  $0.02 - 0.05 \mu\text{m}$  in height[3], with the average asperity slopes of less than one degree, while the size of Cancellous bone asperities range from  $0.1 \mu\text{m}$ , measured from peak to valley, to several tens of micrometers[3]. In this work, both contacting surfaces, i.e. Cancellous bone and Titanium Alloy, initially were of the same surface roughness. Surface topography of both the harder femoral stem and the softer cancellous bone components was modelled by triangular-shape asperities, as illustrated in Figure 2. The assumption of similar surface roughness allowed full interlocking contact between the two asperities to be modelled.

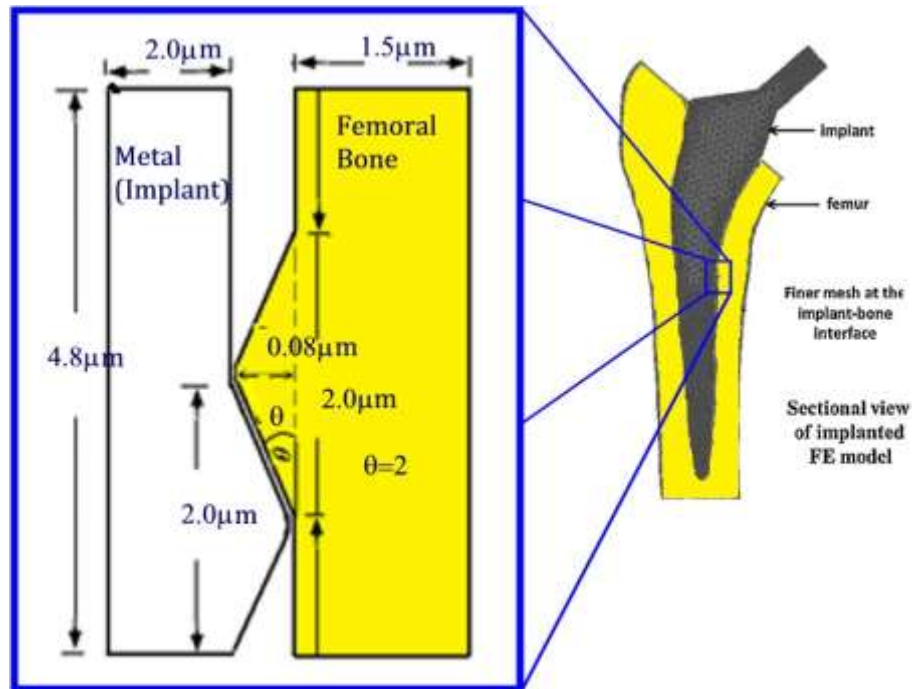


Figure 2: Schematic illustration of the contacting asperities in total hip joint replacement model (*the scale does not represent the correct ratio of vertical to horizontal dimensions*)

As shown in Figure 2, it was assumed that each asperity side-face is in contact with a side-face of the matching asperity, i.e. forming a micro-scale asperity contact. The height of the asperities modelled was  $0.08 \mu\text{m}$  with base angle of  $\theta = 2^\circ$  (the asperity height to width ratio is 0.035). The values of the asperity slope, height and width were chosen with the aim to study the failure mechanisms affected by stresses and deformations during sliding contact, with geometrical dimensions being within the size range of the real head and cup asperities. Asperity base angle of  $\theta = 2^\circ$  was used instead of  $\theta = 1^\circ$  or less in order to study the interlocking effect on the stress and strain changes in the softer asperity.

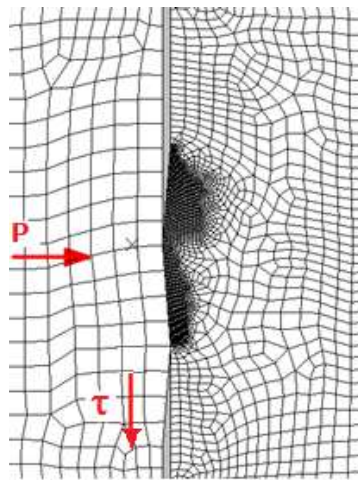


Figure 3: 2-D finite element geometrical model of contacting asperities

For simplicity, a 2-D finite element model was used to simulate the asperity contact. The model was developed using a commercially available FEM package ABAQUS (version 6.3, HKS Inc. U.S.). The contacting asperities were modelled with four-noded plane strain elements as shown in Figure 3.

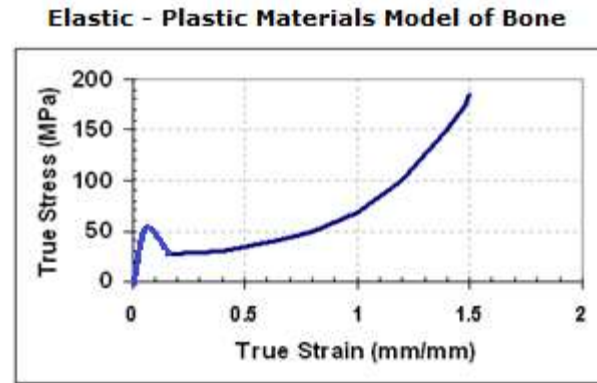


Figure 4: Stress-strain curve of Cancellous Bone used in the model developed [33, 34]

## 2.2. Material Model

Elastic-plastic material behaviour was proposed. It was assumed that the material starts to deform plastically when its yield point reached, i.e.  $\frac{12}{7}\sigma_Y$ , as the material starts to flow plastically when its flow stress is reached, i.e.  $\sigma_f = \frac{12}{7}\sigma_Y$  [35]. In the model proposed the values of plastic yield stress, true stress and true strain at the cancellous bone breaking point were set as 19 MPa, 185 MPa and 1.5 mm/mm, respectively [33]. The stress-strain curve for cancellous bone used in the finite element model is shown in Figure 3 [33], while the material characteristics are listed in Table 1 [34, 36].

Table 1: Mechanical characteristics of materials used in the finite element analysis[34, 36]

Material	Properties		
	Elastic modulus (GPa)	Poisson ratio	Density (kg/m <sup>3</sup> )
Cancellous (femoral bone)[36]	1.0	0.40	950
Titanium Alloy(stem)[34]	208.0	0.30	7800

## 2.3. Loading and Boundary Conditions

The contact between the two surfaces was established first by moving the harder femoral head asperity in the vertical direction onto the fixed softer bone surface to give an initial load. The Titanium AlloysFemoral stem asperity was then moved in the vertical direction, cyclic sliding of micro-motion along the Cancellous bone asperity with a speed of 0.2 ms<sup>-1</sup>. This sliding speed was used in the frictional characterization of explanted Charnley hip prostheses[32]. The vertical sliding results in the higher contact stress at the asperities shown in Figure 3, causing the softer asperity to change its behaviour from elastic through elastic-plastic to fully plastic. The verticalmicro-motion or micro-sliding distance, used in the simulations, was chosen to ensure that the harder sliding asperity (Titanium Alloy stem) had completely passed over the softer fixed asperity (Cancellous bone). The loading and boundary conditions in this model are set in such a manner that the tangential load intensifies as the micro-sliding distance increases. The graph of the contact force changes occurring within the sliding contact is shown in Figure 5.

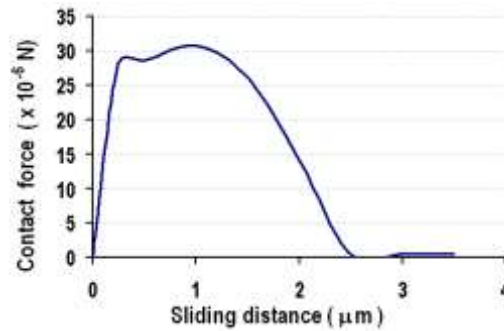


Figure 5: Plot of contact force vs. sliding distance

The effect of friction coefficient was examined with values of 0.8 used in this study. A friction coefficient of 0.8 was assumed to represent a sliding contact between Titanium Alloy and cancellous bone in a total hip joint arthroplasty.

#### 2.4. Material failure in a strain discontinuity approach

The concepts of material failure in discontinuity settings have been reported in several studies[37-40]. The aim of these studies was to identify the mechanisms of material failure and to quantify corresponding critical structural response. It was suggested that material failure (i.e. crack development) usually occurs when the displacement discontinuities take place[25, 37]. Material fracture processes can be categorized into three distinct zones – diffuse failure, weak discontinuity and strong discontinuity zones[37]. The diffuse failure zone is denoted by an increase in strain concentration in a continuous fashion, without the appearance of material discontinuities. The weak discontinuities zone is characterized by a rapid increase in the strain field, resulting in a narrow strain band which exhibits strain discontinuities, however, the displacement field remains continuous. The strong discontinuities zone is defined as the development of the weak discontinuity zone into a band, where the displacement experiences a real jump (discontinuity) and unbounded strain[37].

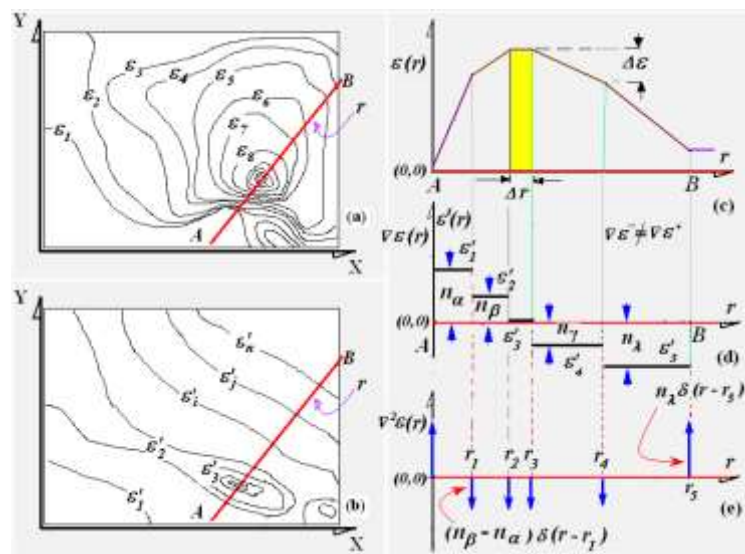


Figure 6: Schematic illustration of discontinuities concept (a) strain field; (b) strain gradient field; (c) cross-section of strain field; (d) cross-section of strain gradient field (with discontinuities); (e) magnitude of strain discontinuities[41]

The discontinuity concept used in this work is based on the discontinuity state of the equivalent plastic strain, which is derived from the rate of change of the equivalent plastic strain with respect to geometrical position. The magnitude of the strain discontinuity itself is obtained from the second derivative of equivalent plastic strain field with respect to the spatial position, as illustrated in Figure 6. Since no prior assumptions regarding the type of material failure (in terms of strain discontinuity settings) are made in modelling of the contact between the two surfaces, the material can be categorized into both diffuse failure zones and weak discontinuity zones. Therefore, a fully conventional finite element method could be implemented in this study in calculating the strain discontinuity fields.

In the narrow band of the continuous strain field zone, the derivation of the strain field with respect to the geometrical position becomes discontinuous across the limits of a narrow band (strain-gradient localization band). In order to observe the magnitude of finite plastic strain discontinuity jumps, it is necessary to examine the point-wise behaviour of the finite plastic strain discontinuity derivation. It can be seen from Figure 5, that  $n_\alpha$ ,  $n_\beta$  or  $n_\gamma$  are constants or the gradients of  $\varepsilon(r)$  and that the delta functions approach the origin from either side [42]. The significance of the sequence  $\nabla^2 \varepsilon(r)$  is relatively easy to interpret. If  $f(r) = \nabla \varepsilon(r)$  and  $f'(r) = \nabla^2 \varepsilon(r)$ , then mathematical descriptions for the strain discontinuity derivative along section AB (Figure 6c), between  $r_0$  and  $r_5$  are:

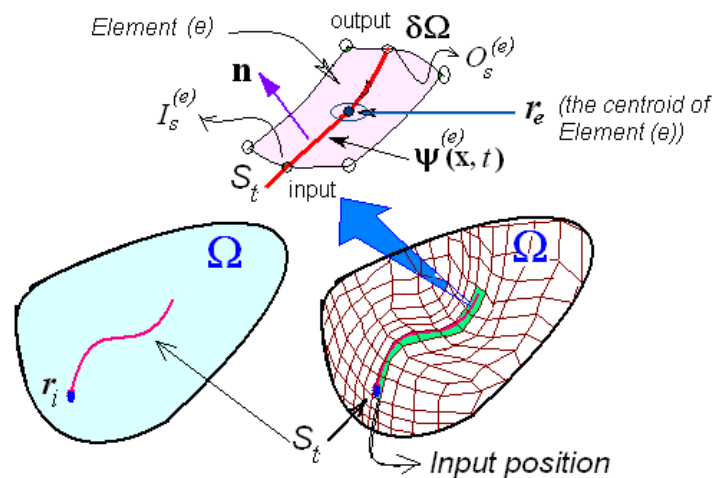


Figure 7: Schematic illustration of 2-D domain with a discontinuity tracking[41]

$$f(r) = \begin{cases} n_\alpha & \text{for } r_0 \leq r < r_1 \\ n_\beta & \text{for } r_1 \leq r < r_2 \\ \dots & \dots \quad \dots \\ n_\gamma & \text{for } r_4 \leq r < r_5 \\ n_\lambda & \text{for } r_5 \leq r < r_6 \end{cases} \quad (1)$$

$$f'(r) = \begin{cases} n_\alpha [\delta(r-r_0) - \delta(r-r_1)] \\ n_\beta [\delta(r-r_1) - \delta(r-r_2)] \\ \dots \\ n_\gamma [\delta(r-r_4) - \delta(r-r_3)] \\ n_\lambda [\delta(r-r_5) - \delta(r-r_4)] \end{cases} \quad (2)$$

Equation (2) can also be presented in the following form:

$$f'(r) = n_\alpha \delta(r-r_0) + (n_\beta - n_\alpha) \delta(r-r_1) + \dots + (n_\gamma - n_\lambda) \delta(r-r_4) + \dots \quad (3)$$

The equivalent plastic strain discontinuities are identified based on the calculation of invariants or components at elements common to two or more other elements; then they are compared to determine the greatest difference (discontinuity jump). The elements that are receiving equivalent values of plastic strain from all nearest elements will exhibit a zero value in a plot of the equivalent plastic strain discontinuities  $f(r) = \nabla \varepsilon(r) = 0$ .

The strain discontinuity, in simple cases, can be used as the criterion of a local failure. The onset of discontinuity also relates to the end of the elastic regime in the bulk material through the fulfilment of some yield or damage criterion[40]. The propagation direction of material failure (on empirical basis) is made orthogonal to the maximum tensile stress[43].

Based on strain discontinuities, it is assumed that a 2-D body  $\Omega$  experiences discontinuities along a discontinuity path,  $St$ , which is characterized by its root  $r$ , i.e. the first nodal point (in the finite element context this is the first element) as schematically illustrated in Figure 6. It is also assumed that for each  $x$  of  $\Omega$  (i.e. every element in the finite element mesh) a propagation direction  $\mathbf{A}^{(e)}(\mathbf{x}, t)$ , orthogonal to the normal  $\mathbf{n}$  to the discontinuity path, is available at every time of the analysis  $\mathbf{A}^{(e)}(t)$  [37].

Prediction of the root of discontinuity propagation location is based on the geometrical region where large-magnitude of finite strain discontinuity jumps (the difference between strain gradients, e.g.  $(n_\alpha - n_\beta)$  etc.) are accumulated. Estimation of the material failure propagation path is made by identifying the tracking line of the displacement of the high finite strain discontinuity jumps to new geometrical positions[41]. Detailed displacement track of accumulating finite strain discontinuity jumps is shown in Suhendra and Stachowiak work[41].

Since the asperities were arranged in an interlocking position, it was assumed that material failure could originate at the base of the softer asperity of the cancellous bone part. Material failure has been associated with a local specific behaviour of the nodal points involving the progressive softening of the material response that spreads across the body and leads to the structural failure. The variation of tensile fracture direction due to loads imposed on the asperity of the softer material, i.e. cancellous bone, is the key issue in this approach aiming to predict the crack initiation and wear particles generated. The direction of tensile fracture occurring in the softer material was examined by the standard continuum mechanics approach, i.e. strain vs. stress non-linear constitutive equations. It is well known that the inclusion of strain-softening features in this approach leads to the strain-

localization phenomenon, in which the strains concentration is confined to a narrow band[37, 38]. This approach, based on the implementation of the plastic strain discontinuities in the model, might be helpful in predicting the mechanisms involved in wear particle formation. The strain discontinuities are understood here as jumps in the strain field experienced by solid materials during deformation (strain) processes[41].

Characterization of material failure has usually been performed by means of local strain with high discontinuity jump concepts. Local failure at a nodal point or at a discrete set of points progresses through the body along failure surfaces in the form of cracks or shear bands [37]. The accumulation of strain discontinuities in a narrow band is responsible for an increasing dissipation of strain energy, and can then be treated as an initial local failure which eventually manifests itself in a form of physically observable propagating surface failure exhibiting a discontinuity in the displacement field [38]. Therefore, strain discontinuities accumulation in the surface layer of contacting bodies can be also treated as an initial process of wear particle formation. The narrow bands of strain concentration, addressed in this study, can prove to be a useful tool in the prediction of wear particle generation mechanisms occurring in joint prostheses.

### 3. Results and discussion

Results obtained from the model developed consist of equivalent (von Mises) stress, equivalent plastic strain, strain energy and plastic strain discontinuity. Based on these results, the possibility of predicting the characteristics of the wear particles generated (e.g. size and shape) is discussed.

#### 3.1. Von Mises stress

The distribution of equivalent von Mises stress field in the subsurface of cancellous bone asperity is shown in Figure 8. The friction coefficient and sliding speed applied in the simulation were 0.8 and 0.2 ms<sup>-1</sup>, respectively.

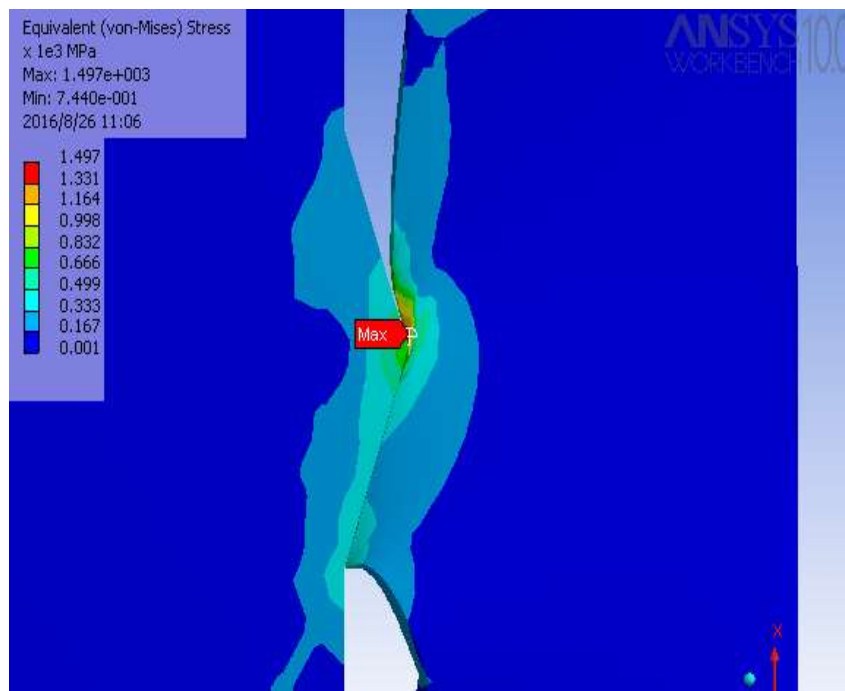


Figure 8: Distribution of equivalent von Mises Stress

The von Mises stress distribution, shown in Figure 8, illustrates how the stress pattern changes as the sliding distance increases. It can be seen from Figure 8 that as the harder Femoral stem asperity slides along the cancellous bone surface, the geometrical position of the highest value of von Mises stress in the cancellous bone subsurface also moves. In addition, as the sliding distance increases, the von Mises stress value raises from 26.3 MPa at the initial position to 33.1 MPa at a sliding distance of  $3.0\mu\text{m}$ . As the tangential force increases with the displacement, the maximum shear stress value repositions itself closer to the interface/surface. It might be assumed that the possible degradation of Cancellous bone asperity, leading to crack development, may take place in the region where the highest values of von Mises equivalent stress occur.

### 3.2. Equivalent plastic strain

The surface and subsurface deformation of the softer asperity during loaded sliding contact was also examined. The surface stress change and internal equivalent plastic strain field in the deformed cancellous bone asperity occurring during contact under the friction coefficient of 0.8 are shown in Figure 9. It can be seen from Figure 9 that the geometrical position of the maximum value of equivalent plastic strain in the cancellous bone asperity moves during sliding.

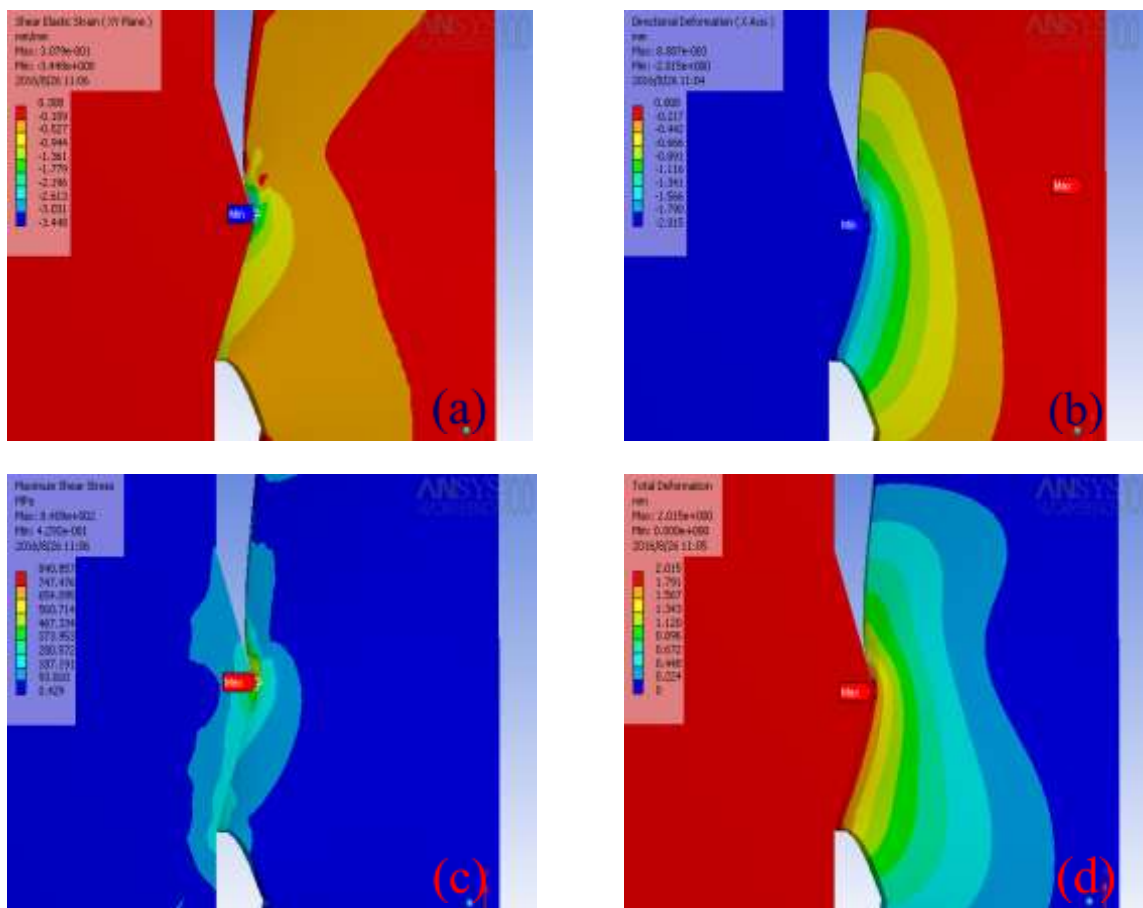


Figure 9: (a) Shear Elastic Strain; (b) Directional Deformation; (c) Maximum Shear Stress; (d) Total Deformation

As the sliding contact moves across the surface of the THR (between the Stainless steel Femoral stem and cancellous bone) much of the damage done to the softer material occurs beneath the micro-sliding surface. Cyclic plastic deformation occurs across the softer asperity surface area as the harder

asperity passes over the surface and the frictional traction forces increase the plastic deformation[44]. Although internal strain in the softer material may eventually attain extremely high levels, it does not directly contribute to crack growth unless it is accompanied by an internal triaxial compressive stress field that occurs directly beneath a contacting asperity [45].

### 3.3. Plastic strain discontinuity

The location where the initial crack (material's failure) may occur in the softer asperity has been examined based on the von Mises stress field behaviour (Figure 7). Real wear processes are complex, as many factors are involved in the formation of a wear particle occurring between the articulating surfaces of THR [33]. Nevertheless, plastic strain discontinuity examination gives information that might prove to be useful in the prediction of wear particle detachment and formation.

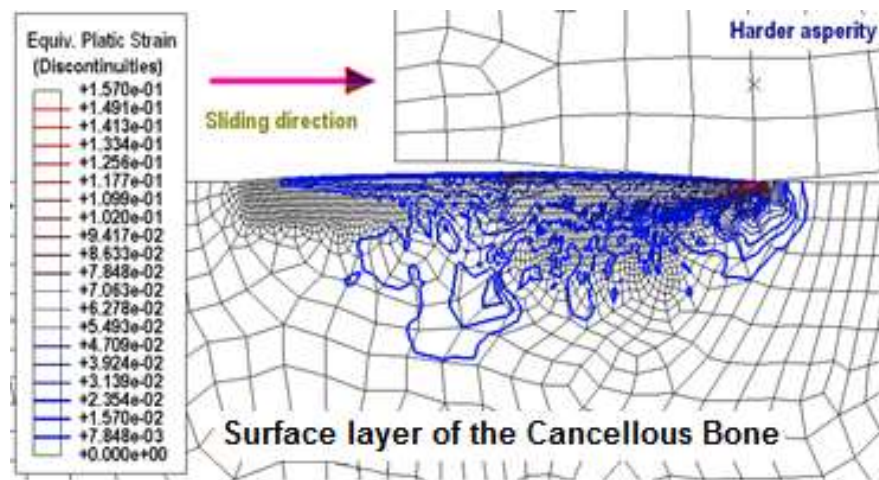


Figure 9: Fields of equivalent plastic strain discontinuities in the cancellous bone asperity subsurface with friction coefficient of 0.8 and sliding speed of 0.2 ms<sup>-1</sup>

Some of the continuum mechanical models of solids allow for the formation of surface strain discontinuities when the body is deformed. Across such a deforming surface, the stress and strain fields suffer finite discontinuity jumps even though the traction and displacement fields remain continuous. The fields of equivalent plastic strain discontinuity in the cancellous bone asperity subsurface with friction coefficient of 0.8 and sliding speed of 0.2 ms<sup>-1</sup> are shown in Figure 9. It can be seen from Figure 9 that plastic strain discontinuity occurs in the subsurface of cancellous bone asperity close to its surface. The strain discontinuity was observed at sliding distance of 1.35  $\mu$  m when the strain energy reaches its highest value.

## 4. Conclusions

From the study conducted the following conclusions can be drawn:

- The model of a loaded sliding contact between two asperities has been developed. The calculation results confirmed that the positions of maximum plastic strain and von Mises stress depend on the friction coefficient and the magnitude of load applied.
- As the friction coefficient and sliding contact force increase, the maximum von Mises stress and plastic strain are moving closer to the surface.
- The evolution of equivalent von Mises stress and equivalent plastic strain within the polyethylene, resulting from a frictional sliding contact, might be useful in interpretation of wear particle detachment mechanisms in tough polymers, like cancellous bone.

- The strain energy as well as the strain discontinuity generated might be of use in the prediction of wear particle formation.
- The friction coefficient has a significant effect on the stress and strain state occurring between the contacting asperities, as well as on the area subjected to higher stress and strain states.
- Strain discontinuity approach might be a useful tool in prediction of wear particle formation.

## References

- [1] Mow, V.C., A. Ratcliffe, and S.L.Y. Woo, Bio-tribology of synovial joints. Vol. 1. 1990, New York: Springer-Verlag. 323 - 345
- [2] Podsiadlo, P., M. Kuster, and G.W. Stachowiak, Numerical analysis of wear particles from non-arthritis and osteoarthritis human knee joints. *Wear*, 1997. 210(1-2): p. 318-325
- [3] Dowson, D., A comparative study of the performance of metallic and ceramic femoral head components in total replacement hip joints. *Wear*, 1995. 190(2): p. 171-183
- [4] Podsiadlo, P. and G.W. Stachowiak, 3-D imaging of surface topography of wear particles found in synovial joints. *Wear*, 1999. 230(2): p. 184-193.
- [5] Firkins, P.J., et al., A novel low wearing differential hardness, ceramic-on-metal hip joint prosthesis. *J. Biomechanics*, 2001. 34(10): p. 1291-1298.
- [6] Maloney, W.J., et al., Fibroblast response to metallic wear debris in vitro. *J. Bone Jt. Surgery*, 1993. 75A: p. 835 - 844.
- [7] Wirganowicz, P.Z. and B.J. Thomas, Massive osteolysis after ceramic on ceramic total hip arthroplasty. *Clinical Orthop.*, 1997. 338: p. 100 - 104
- [8] Catelas, I., et al., Induction of macrophage apoptosis by ceramic and polyethylene particles in vitro. *Biomaterials*, 1999. 20(7): p. 625-630.
- [9] Panichkul, P., et al., New Approach and Stem Increased Femoral Revision Rate in Total Hip Arthroplasty. *Orthopedics*, 2016(1): p. 86 - 92.
- [10] Goodman, S.B., Huie, P., Song, Y. P., Schurman, D., Maloney, W., Woolson, S., Sibley, P., Cellular profile and cytokine production at prosthetic interfaces. *J. Bone Jt. Surgery*, 1998. 80: p. 531 - 539.
- [11] Verdonchot, N., E. Tanck, and R. Huiskes, Effects of prosthesis surface roughness on the failure process of cemented hip implants after stem-cement debonding. *J Biomed Mater Res*, 1998. 42: p. 554 - 559.
- [12] Chiba, J., et al., Biochemical analyses of human macrophages activated by polyethylene particles retrieved from interface membranes after failed total hip arthroplasty. *J. Arthroplasty*, 2001. 16(8): p. 101 - 105
- [13] Kobayashi, A., Freeman, M. M., Bonfield, W., Number of polyethylene particles and osteolysis in total joint replacements: Quantitative study using a tissue-deggestion method. *J. Bone Jt. Surgery*, 1997. 14: p. 840 - 873.
- [14] Green, T.R., Fisher, J., Stone, M., Wroblewski, B. M. and Ingham, E., Polyethylene particles of 'critical size' are necessary for the induction of cytokine by macrophages in vitro. *Biomaterials*, 1998. 19(24): p. 2297 - 2302.
- [15] Oparaugo, P.C., et al., Correlation of wear debris-induced osteolysis and revision with volumetric wear-rates of polyethylene: A Survey of 8 reports in the literature. *Acta Orthop. Scand.*, 2001. 72(1): p. 22 - 28.
- [16] Collis, D. and C. Mohler, Comparison of clinical outcomes in total hip arthroplasty using rough and polished cemented stems with essentially the same geometry. *J Bone Joint Surg Am*, 2002(84): p. 586 - 592.
- [17] Herberts, P., H. Malchau, and G. Garellick, Annual report 2003. The Swedish National Hip Arthroplasty Register, 2004.
- [18] Lancaster, J.G., et al., The wear of ultra-high molecular weight polyethylene sliding on metallic and ceramic counterfaces representative of current femoral surfaces in joint replacement.

- Proc. Instn. Mech. Engrs. (H) J. Eng. Med., 1996. 211(Part H): p. 17 - 24.
- [19] 19. Harris, W., J. McCarthy, and D. O'Neill, Femoral component loosening using contemporary techniques of femoral cement fixation. *J Bone Joint Surg Am*, 1982. 64: p. 1063 - 1067.
  - [20] Taylor, M. and T. KE, Fatigue failure of cancellous bone: a possible cause of implant migration and loosening. *J Bone Joint Surg Br*, 1997. 79: p. 181 - 182.
  - [21] Tipper, J.L., et al., Characterisation of wear debris from UHMWPE on zirconia ceramic, metal-on-metal and alumina ceramic-on-ceramic hip prostheses generated in a physiological anatomical hip joint simulator. *Wear*, 2001. 250(1-12): p. 120-128.
  - [22] Hall, R.M., et al., The association between rates of wear in retrieved acetabular components and the radius of the femoral head. *Proc. Instn. Mech. Engrs. (H) J. Eng. Med.*, 1998. 211: p. 321 - 326.
  - [23] Learmonth, I.D. and J.L. Cunningham, Factors contributing to the wear of polyethylene in clinical practice. *Proc. Instn. Mech. Engrs. (H) J. Eng. Med.*, 1997. 211(Part H): p. 49 - 57.
  - [24] Hall, R.M., et al., The effect of surface topography of retrieved femoral heads on the wear of UHMWPE sockets. *Medical Eng. & Physics*, 1997. 19(8): p. 711-719.
  - [25] Suhendra, N., Computational analysis for prediction of loaded sliding contact effects in total hip joint prosthesis, in *Proceeding of the 3th International Biomaterials Conference*, I.N. Jujur, Editor. 2014, BIOMAT 2014: Surabaya - Indonesia.
  - [26] McNie, C., et al., Prediction of plastic strain in ultra-high molecular polyethylene due to microscopic asperity interactions during sliding wear. *Proc. Instn. Mech. Engrs. (H) J. Eng. Med.*, 1998. 212(Part H): p. 49 - 56.
  - [27] Adams, G.G. and M. Nosonovsky, Contact modeling -- forces. *Tribology Intl.*, 2000. 33(5-6): p. 431-442.
  - [28] Stachowiak, G.W., Friction and Wear of Polymers, Ceramics and Composites in Biomedical Applications, in *Advances in Composites Tribology*, K. Friedrich, Editor. 1993, Elsevier: Amsterdam. p. Chapter 14: 509-557.
  - [29] Cooper, J.R., D. Dowson, and J. Fisher, Birefringent studies of polyethylene wear specimens and acetabular cups. *Wear*, 1991. 151(2): p. 391-402.
  - [30] Scholes, S.C., S.M. Green, and A. Unsworth, The wear of metal-on-metal total hip prostheses measured in a hip simulator. *Proc. Instn. Mech. Engrs. (H) J. Eng. Med.*, 2003. 215(Part H): p. 523 - 530.
  - [31] Vassiliou, K. and A. Unsworth, Is the wear factor in total joint replacements dependent on the nominal contact stress in ultra-high molecular weight polyethylene contacts? *Proc. Inst. Mech. Engr. (H) J. Eng. Med.*, 2004. 218: p. 101 -- 107.
  - [32] Fisher, J., Dowson, D., Hamdzah, H. and Lee, H. L., The effect of sliding velocity on the friction and wear of UHMWPE for use in total artificial joints. *Wear*, 1994. 175(1-2): p. 219-225.
  - [33] Kurtz, S.M., Pruitt, L., Jewett, C. W., Crawford, R. P., Crane, D. J., Edidin, A. A., The yielding, plastic flow, and fracture behavior of ultra-high molecular polyethylene used in total joint replacements. *Biomaterials*, 1998. 19: p. 1989 - 2003.
  - [34] Anoname. In: Matweb (Material Property Data), BioDur Carpenter CCM Alloy. Data alloy [online]. Available from: <http://www.matweb.com/search/SpecificMaterial.asp?bassnum=NCAR40>. [cited [Accessed 25 July 2004].BioDur Carpenter CCM Alloy. Data alloy [online].
  - [35] Kaliszky, S., Plasticity: Theory and Engineering Applications. *Studies in Appl. Mech. Vol. 21*. 1989, New York: Elsevier Science Publishing Company, Inc. 505.
  - [36] Jin, Z.-M., A general axisymmetric contact mechanics model for layered surfaces, with particular reference to artificial hip joint replacement. *Proc. Instn. Mech. Engrs. (H) J. Eng. Med.*, 2000. 214(Part H): p. 425 - 435.
  - [37] Oliver, J., On the discrete constitutive models induced by strong discontinuity kinematics and continuum constitutive equations. *Intl. J. Solids Struct.*, 2000. 37(48-50): p. 7207-7229.

- [38] Sukumar, N. and J.-H. Prevost, Modeling quasi-static crack growth with the extended finite element method Part I: Computer implementation. *Intl. J. Solids Struct.*, 2003. 40(26): p. 7513-7537.
- [39] Wells, G.N. and L.J. Sluys, Application of embedded discontinuities for softening solids. *Eng. Fract. Mech.*, 2000. 65(2-3): p. 263-281.
- [40] Wells, G.N. and L.J. Sluys, A new method for modelling cohesive cracks finite element. *Intl. J. Numer. Method. Eng.*, 2001. 50: p. 2667 - 2682.
- [41] Suhendra, N. and G.W. Stachowiak, Computational model of asperity contact for the prediction of UHMWPE mechanical and wear behaviour in total hip joint replacements. *Tribology Letters*, 2007. 25(1): p. 9 - 22.
- [42] Hoskins, R.F., *Generalised Functions. Mathematics and its applications*, ed. G.M. Bell. 1979, London: Ellis Horwood Limited (Div. John Wiley & Sons).
- [43] Pradeilles - Duval, R.-M. and C. Stolz, Mechanical transformations and discontinuities along a moving surface. *J. Mech. Phys. Solids*, 1995. 43(1): p. 91 - 121.
- [44] Edidin, A.A., et al., Plasticity-induced damage layer is a precursor to wear in radiation-cross-linked UHMWPE acetabular components for total hip replacements. *J. Arthroplasty*, 1999. 14(5): p. 616 - 627.
- [45] Krzypow, D.J. and C.M. Rimnac, Cyclic steady state stress-strain behavior of UHMW polyethylene. *Biomaterials*, 2000. 21(20): p. 2081-2087.
- [46] Oliver, J. and A.E. Huespe, Continuum approach to material failure in strong discontinuity settings. *Comp. Meth. Appl. Mech. Eng.*, 2004. 193(30-32): p. 3195-3220.

### Acknowledgments

The author wish to thank Ministry for Research and Technology in the scheme of Incentive Programme of Applied Research for their financial support and Agency for the Assessment and Application of Technology, Centre for Materials Technology for its help during the preparation of this paper. Thanks to THA team members for the very good collaboration as a team work. Thanks also to Professor Gwidon Stachowiak for his inspiration from beginning the writer worked in Tribology Laboratory at UWA – Australia until presently.